

Influence of Surface Pitting and Friction Coefficient on the Static Transmission Error in Spur Gears

Iqbal Shareef

Department of IMET, Bradley University, Peoria, Illinois, USA
Email: shareef@bradley.edu

Timothy L. Krantz and Wasiq A.M Abdul

NASA Glenn Research Center, Cleveland, Ohio, USA
Dept of IMET, Bradley University, Peoria, Illinois, USA
Email: timothy.l.krantz@nasa.gov and wasiq.emerald@gmail.com

Abstract—This research studies the performance characteristic, *Static Transmission Error (STE)*, of a spur gear pair rotating under friction with and without damage in the form of a pit on gear teeth. Using a profilometer scan of a pit from an aerospace test gear, a damage shape in the form of parabolic profile pit is simulated on the surface of tooth of spur gear at seven different locations having three different sizes of the damage profile depth. Using the measured pit depth from profilometry, two additional pit depths were simulated by multiplying the initial profile depth by 5, and then by 10, for a total of three different profile depths having the same pit width. Similarly, six different coefficients of friction starting from zero to a maximum of 0.30 in the intervals of 0.06 were investigated. The combination of seven different locations of pits, six friction coefficients, and four pit depths resulted in a total of 168 unique combinations. Analyses were completed and multiple outputs responses including the STE were recorded, but only STE results are presented in this paper. Results show that STE variation increases with increase in friction coefficient and the size of damage.

Index Terms— static transmission error, tooth surface pitting, coefficient of friction, tooth load, contact pressure

I. INTRODUCTION

Gears are one of the most common mechanical components that are used for transmission of power in a large variety of mechanical devices. Other key roles played by gears include speed reduction in motorized equipment or adjust the direction of rotation in differentials to transmit power in automobiles. While transmitting power, tooth undergo bending and deflection. Bonori et al., [1] described tooth deflection as another source of noise and vibration in the gears due to resulting transmission error. Chaari et al., [2] discussed the

excitation in noise and vibration is highest when the gears are operated in poor mechanical conditions such as improper lubrication, teeth damage, teeth faults, spacing errors etc. A scan of literature shows extensive research done on gear noise and vibration in the last 3 decades [3-9]. The normal operating condition of gears are affected due to presence of defects which decrease the efficiency of transmission, and consequently result in catastrophic transmission failure causing the entire system to halt. Hbaieb et al., [10] described tooth surface pitting are the most common damage in gears resulted from gear deflections under load.

Randall [11] described a method to identify the type and location of the developing fault in the gearbox with the help of studying the changes in the vibration signal measured externally on continuously operating gearboxes. The study was based on the interpretation of change in the frequency spectrum of the vibration signals. McFadden [12] examined the time domain average of the vibration produced by meshing gears with application to early detection of gear failure and found that the tooth meshing harmonics extracted from the time domain average of vibration of a complete gear actually defines the time domain average of the meshing vibration of a single gear tooth. McFadden [13] extended the amplitude and phase modulation technique of extracting the vibration signal to identify the fault in the gear by showing the relation between phase angle of the change in the vibration and location of the crack in the tooth to identify the fatigue crack. This method was demonstrated by analysis of vibration of a spiral bevel gear with a fatigue crack at the root of one of the teeth.

Zakrajsek et al., [14] used three different vibration diagnostic techniques to detect the gear tooth fracture in high contact ratio face gear mesh. The methods used average signal in both time and frequency domains. They found that all the methods used were able to detect the gear tooth failures along with surface pitting and severe wear. Choy et al., [15] simulated and analyzed the vibration in the gear transmission system with various

Manuscript received October 25, 2019; revised January 1, 2020.

This material is declared a work of the U.S. Government, is not subject to copyright protection in the U.S., and is approved for public release.

failures including surface pitting, wear, and partial tooth fracture of the gear teeth. They introduced the Wigner Ville distribution to examine the gear vibration in the joint time-frequency domain for vibration pattern recognition. Kuang and Lin [16] studied the effect of tooth wear on the vibration spectrum variation of a rotating spur gear pair by considering load sharing alternation, position dependent mesh stiffness, damping factor and friction coefficient to approximate dynamic characteristics of an engaging spur gear pair.

Dempsey [17] used oil debris sensor to predict the gear pitting damage on the spur gear pair. The study included collection of data from 8 different experiments using no damage and pitting damage gear pair. The data was used to identify the membership functions to build a simple fuzzy logic model, and it was found that the fuzzy logic technique with oil debris accumulated mass is a good predictor for pitting damage on spur gears.

Howard, Jia, and Wang [18] studied the effect of friction, and presence of crack in a spur gear pair mesh, by using MATLAB and Simulink models developed from the differential equations to compare data for without friction and with friction. Decker [19] proposed two new gear crack techniques using tooth analysis by improving existing techniques. After careful analyses of the two new techniques Decker concluded that the developed techniques still do not have enough robustness and accuracy and it is impossible to be able to reliably detect a tooth fracture in sufficient time to be able to monitor its growth. Liu and Pines [20] developed an analytical model to simulate the gear mesh contact for a spur gear pair with and without damage. The damages considered were pitting, wear and root cracks to study the static performances, and found that the basic gear design parameters may have significant effect on damage detection sensitivity. Results show that decrease in diametrical pitch will enhance damage detection sensitivity for pitting, wear, and root cracks, whereas increase in pressure angle or number of teeth will enhance detection sensitivity for pitting damage but this was opposite in the case of crack and wear damage.

Endo, and Randall [21] studied the static analysis of spall on tooth flank and crack in the tooth fillet region and developed a technique to differentially diagnose the faults. Chaari, Fakhfakh and Haddar [22] utilized the Wigner-Ville distribution to compare the dynamic response of a healthy planetary gear and response of planetary gear containing tooth defects in both time and frequency domains, and in the joint time frequency domains. Hbaieb et al., [23] discussed the dynamic effects of eccentricity, profile errors, and tooth pitting occurring during running of a planetary helical gear mesh.

In this research the effect of damage severity, as quantified by pit depth, in the presence of friction is studied using a series of linear elastic static analysis. The study used four different pit sizes at seven different locations for each of six different coefficients of frictions, resulting in a total of 168 unique combinations of friction, pit size, pit depth, and pit location. Using a measured pit profile obtained by profilometer inspection of a damaged

tooth, the pit shape was modeled. Several output responses were calculated but only the Static Transmission Error (STE) results are shown in this study.

II. GEAR DESIGN PARAMETERS AND TOOTH DAMAGE

The spur gear parameters used in this study are described in Table 1, and as schematic of the gear pair is shown in Figure 1. This was chosen for study as the gear pair could be studied using the authors' laboratory equipment for purposes of experimental validation studies.

TABLE I. GEAR DESIGN PARAMETERS

Gear/Pinion Parameters	Dimensions
Number of Teeth	28
Pitch Circle Diameter (mm)	88.9
Diametral Pitch (teeth/mm)	0.315
Module (mm/tooth)	3.175
Circular Pitch (mm)	9.975
Pressure Angle (Degrees)	20
Addendum (mm)	3.175
Tooth Thickness (mm)	4.813
Hob Tip Radius (mm)	1.02
Outer Diameter (mm)	95.2
Root Diameter (mm)	79.8
Inner Diameter (mm)	25.4
Gear Blank Thickness (mm)	6.35
Face Width (mm)	5.334
Young Modulus (GPa)	207
Poisson's Ratio	28

The boundary conditions used for the analysis of this study included the gear inner diameter fixed from rotating while the torque is applied to the pinion inner diameter. Both the gear and pinion inner diameters are constrained as rigid circles. The inner diameter rigid circles lateral degrees of freedom were constrained to ground via a bearing stiffness matrix having a stiffness value of 876 kN/mm. The material response was linear-elastic, and the fillet root stresses were determined using plane stress analysis.

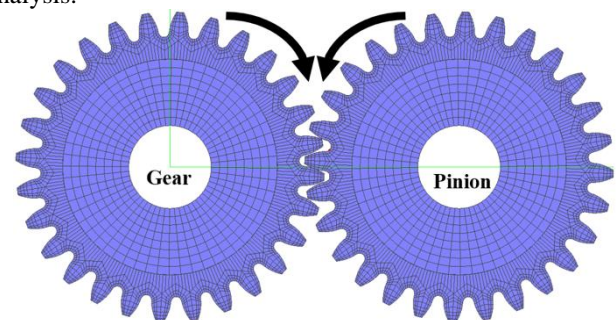


Figure 1. Spur gear pair

All studies were done for an input torque of 621.4 N-m (5,500 in-lb). This torque was chosen for the study to

create contact pressures matching that used by NASA for accelerated testing of gear contact fatigue lifetimes. The analyses were static solutions for a series of ‘time-steps’. For each time-step, the pinion and gear are rotated according to the kinematics, and as per the specified pinion speed. The speed was selected so that a time increment of 1.00 second corresponds to a rotation of one tooth pitch. At time equal to 0.00 seconds, an undeformed pinion tooth, and the corresponding mating gear tooth make contact at the pitch point. A time-step size of 0.05 seconds was used in this investigation.

A. Gear Tooth Damage

There are various types of gear tooth damages that can affect the process of power transmission such as wear, cracks, surface pitting and fatigue damage etc. In this research the effect of tooth surface pitting on the performance characteristics of involute spur gear pair is investigated. The pits can occur at the pitch point, and on either sides of pitch point with various shapes and sizes depending on the depth of the initial fracture and how far the pitting has progressed. Fig. 2 shows examples of damages to gear teeth surfaces of differing severity. Fig. 2(a) is an example of minor pitting damage comprising of small surface pits, while 2(b) shows more extensive damage with larger and deeper pits across the entire active face width. On the other hand, Fig. 2(c) and 2(d) are examples of minor and major scuffing damages.

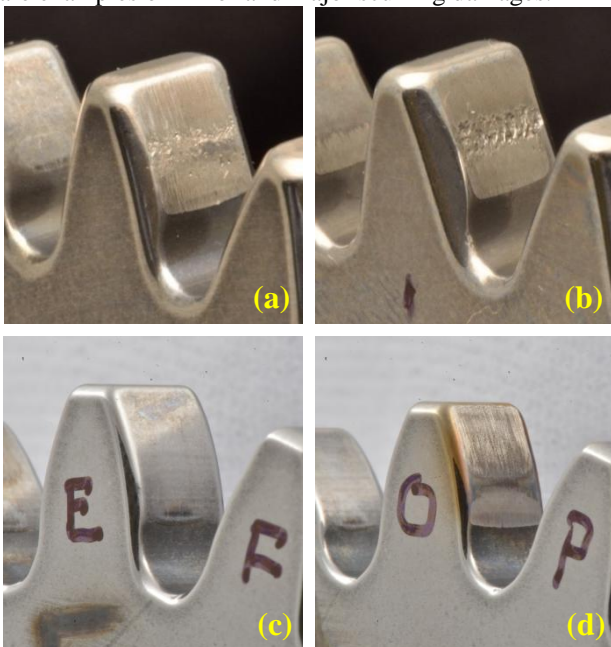


Figure 2. Example of gear damages in the form of pitting and scuffing. (a) initial pitting, (b) large pitted areas spread over gear flank, (c) minor scuffing, (d) severe scuffing with thermal damage.

Using pitted gears from NASA’s gear fatigue tester having damage similar to that of Fig. 2(b), several pits were scanned. Fig. 3 shows a typical stylus profilometer scan of the pit on a gear tooth. The pit is an irregular shape close to the shape of parabola, when approximated with the pit width = 0.4064 mm (0.016”) and pit depth = 0.0127 mm (0.0005”). This being an actual example of a pit from a real-life gear test, served as a motivation for

simulating a pit with the shape of parabola on the tooth surface.

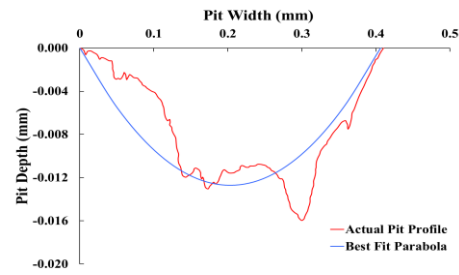


Figure 3. Damage shape approximated.

In this research the simulated pits are placed on tooth number one of the driver gear i.e., on the pinion, at seven different involute profile locations such that the centers of the pits are equidistant from one another regardless of the width and depth of the pit. The first pit is placed such that the center of the pit coincides with the pitch point and three pits at equal distance from one another towards the addendum side and the remaining three at the dedendum side. Fig. 4a shows the locations of pits on the tooth surface. Figure 4b shows the pit size investigated. It can be seen that the pit width is kept constant varying the pit depth ranging from 0 mm (No damage) to a maximum of 0.127 mm (0.005”). By considering the size of pit from Fig. 3 as base i.e., maintaining the pit width = 0.4064 mm (0.016”) as fixed and by increasing the depth in the multiples of 5 and 10 resulting in the three different depths with the magnitude of 0.0127 mm, 0.0635 mm and 0.1270 mm respectively.

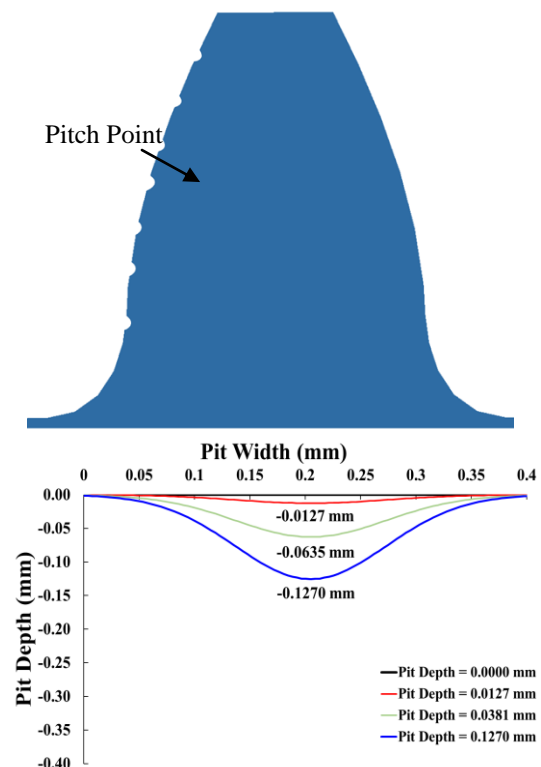


Figure 4. (a) location of Pits on tooth surface (b) Graphical representation of Pit shapes Investigated

B. Effect of Friction

Gear boxes transmitting power include parts having surface in contact to transmit forces. Power transmitting gears can experience wear, and surface fatigue (micro pitting, pitting and spalling). The wear rate and surface fatigue life are highly influenced by the lubricating films and friction condition. In order to reduce the wear and fatigue rates of the gears the coefficient of friction should be as low as possible. The friction condition also influences the transmission error of the gear pair.

This research studied the performance characteristics of involute gear pair in the presence of damage as well as the presence of friction. The different friction coefficients considered are in the range of 0 (no friction) to a maximum of 0.30 in the intervals of 0.06 friction coefficient. The effect of friction shows some interesting features on the performance of gear pair.

The combination of both damage and friction on the static transmission error are studied and are compared in the results section. The study used four different pit sizes at seven different locations for each of six different coefficients of frictions, resulting in a total of 168 unique combinations of friction, pit size, pit depth, and pit location.

III. ANALYSIS PROCEDURE AND PROCESSING OF TRANSMISSION ERROR

A. Numerical Analysis

A two-dimensional finite-element-based multi-body contact analysis algorithm developed by Vijayakar [24] was used for computer simulation of the gear performance. In this simulation no prior assumptions were made about the distribution of forces and contact stresses on the gear teeth. Finite element formulations were used for determining the bending deformations of the gear teeth. Contact deformations and contact stresses on the gear teeth were determined by a combined surface integral/finite element solution. Based on rigid body kinematics with no load applied, candidate points of contact are located, and then a quadratic programming technique was used to solve for contact positions on deformed gear geometries. Figure 1 depicts the finite element model of the gear pair. As required for the numerical contact analysis, specialized surface geometry having nonlinear shapes with established radii of curvatures and accurate orientations of the surface normal vectors were defined for the gear tooth flanks. High order finite elements were used for elements located in the gear root, fillet, and contact surface regions. Figure 1 accurately depicts the finite element mesh corner node locations but does not depict the additional nodes of the high-order finite elements. The mesh density used in this study matches that of Vijayakar [25]. His work established the adequacy of the finite element mesh density. For numerical solution of the contact deformations and pressures, the simulation technique requires not only the definitions of the finite element mesh shown in Fig. 1 but also the specification of contact cells. In this study 37 contact cells having a linear

dimension of 0.0254 mm (0.001 inch) along the profile surface were used. Details of analysis methodology can be found in the work described by Vijayakar [24].

In this research, all simulations have been performed using a numerical approach that has been used by several gear researchers and has been experimentally validated. Krantz [26] using strain gages measured the sun gear, and ring gear root stresses of a helicopter planetary gear system. Using Krantz's [26] results, Vijayakar et al. [25] showed good agreement between analysis results and experimental tooth root stresses in sun gear and ring gear of a helicopter planetary gear system. Using the same approach Ligata et al., [27], and Kahraman, et al. [28] conducted validation experiments of precision planetary gear sets to investigate several system level effects. Their numerical model predictions agreed very well with the measured planet load sharing, hoop strains, and gear rim deflections. Prueter [29], and Prueter et al., [30] used the same method to study a three-stage wind turbine gear system, in which root strains from the ring gears of both planetary stages were compared to the analyses and found good agreement. Ericson and Parker [31] demonstrated good agreement of the method to experiments for planetary system natural frequencies, mode shapes, and dynamic responses. Using the same numerical analysis Parker et al., [32] found good agreement to the experimental work done by Kahraman and Blankenship [33]. Beghini et al., [34], and Tamminana et al., [35] also used the same numerical approach and demonstrated excellent agreement to their dedicated validation experiments. The validation work done by the foregoing authors, served as a motivation to use the same numerical analysis approach for all simulations in this study. The boundary conditions used for the analyses included the gear inner diameter being constrained from rotating, and the torque being applied to the pinion inner diameter. The inner diameters of both gear and pinion were constrained as rigid circles. The lateral degrees of freedom of the gear inner diameters were constrained to ground via a bearing stiffness matrix having a stiffness value of 876 kN/mm. All analyses were static solutions performed for an input torque of 621 N-m (5,500 in-lb) and a time step of 1.0 second corresponding to a rotation of one tooth pitch. At time $t = 0.0$, and load $p = 0.0$, the contact between pinion and gear was at the pitch point. A time-step size of 0.05 seconds was used in this investigation.

B. Post Processing of Transmission Error

Most commonly transmission error (TE) is quantified as a linear dimension along the line-of-action by multiplying the angular displacement in radians with the base circle radius. In this study TE was defined and calculated for analytical simulation as angular displacement in units of radians. By multiplying the angular displacement in radians with the base radius 41.8 mm of the mating gears, the corresponding transmission error in linear dimension was obtained.

As shown in Figure 1 and also listed in Table 1, there are 28 teeth in each of the two mating gears. In order to study the loading effect on each tooth, the driving gear was rotated in such a way that each tooth took exactly

one second from the start of contact till the end of the contact with the mating tooth. A typical plot of transmission error at 621.4 N-m (5,500 in-lb) Torque is shown in Fig. 5, in which TE is shown both in units of radians and micrometers. The abscissa shows a time span of 1 second corresponding to one full contact period of the gear tooth. In Fig. 5 at time $t = -1.0$ seconds the TE is nearly 91 μm , but as the gear rotates, tooth experiences greater force as the contact moves from dedendum side to pitch point and the corresponding TE is 163 μm . Then the load on the tooth begins to decrease as the contact moves from pitch point to addendum side and finally leaves the contact.

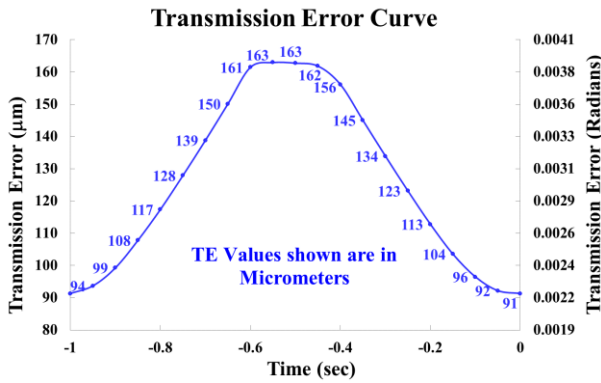


Figure 5. Typical example of a transmission error curve at 621.N-m torque

The static transmission error waveform characteristics were quantified in three different ways: Peak-to-Peak, Root Mean Square, and Total Area of transmission error, which are described in the following.

The *Peak-to-Peak Transmission Error* (PPTE) is the difference in the maximum transmission error and the minimum transmission error measured in a rotation of one tooth pitch. The time of one second in abscissa of the Fig. 5 corresponds to a rotation of one tooth pitch. From Fig. 5 the maximum TE is 162.951 μm (0.00389835 radians) and the minimum TE is 91.279 μm (0.00218372 radians). Thus, the Peak to Peak Transmission Error is then calculated as PPTE = 71.672 μm (0.00171463 radians)

The *Root Mean Square Transmission Error* (RMSTE) is the square root of the arithmetic mean of squares of the difference of the Transmission Error and the mean of all transmission errors.

$$RMSTE = \sqrt{\frac{\sum_{i=1}^n (TE_i - \mu)^2}{n}}$$

For example, in Fig. 5, the mean of all transmission errors is 125.329 μm (0.00299829 radians) and the calculated RMSTE is 26.235 μm (0.00062764 radians).

The *Total Area Transmission Error* (TATE) per cycle is the measure of absolute total area calculated from the mean of the TE variation. In this case after having determined the mean value of the TE as 125.329 μm , Simpson's Rule was applied to find the total area by

summing the areas above and below the mean line. The total area is obtained from the following formula:

$$TATE = \frac{\Delta x}{3} [ATE_1 + 4ATE_2 + 2ATE_3 + 4ATE_4 + \dots + 2ATE_{n-2} + 4ATE_{n-1} + ATE_n]$$

where $ATE_i = |TE_i - \mu|$, and TE_i is the transmission error at point i , $\mu = 125.329 \mu\text{m}$ is the mean of TE_i , in which $i = 1, \dots, n$, where n represents the number of partitions. In this example calculation $n = 20$ and TATE = 23 μm (0.00055108 radians).

Peak-to-Peak Transmission Error (PPTE) and Root Mean Square Transmission Error (RMSTE) are the two common approaches used to find the static transmission error (STE). PPTE and RMSTE are methods in which only the peak-to-peak, or RMS values of the profile are used and not the entire profile of the error signal. To supplement previously used methods (PPTE, RMSTE) which use discrete values of the profile, a new method of STE quantification, Total Area Transmission Error (TATE), was used by calculating the area under the entire error curve. The area under a waveform is a measure of the power associated with the waveform. Therefore, the idea of finding the areas above and below the mean line was used. As this curve is a discrete function of time, Simpson -1/3 method was used.

Graphical representation of how PPTE, RMSTE, and TATE were quantified is shown in Fig. 6. The same three methods were also used by Abdul et al., [36].

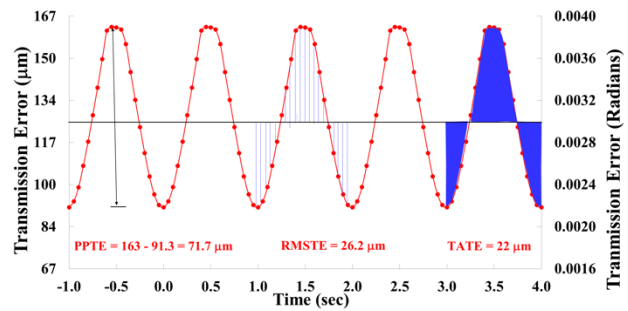


Figure 6. Graphical representation of PPTE, RMSTE, and TATE

IV. RESULTS AND DISCUSSION

The various responses calculated using FEA simulation include static transmission error (STE), tooth loads, root stresses, contact stresses, gear moments, and bearing forces, at four different pit sizes for each of six different coefficients of friction. However, only results of the static transmission error are presented in this manuscript.

STE for different pit sizes and friction coefficients is shown in Figure 7 for rotation duration of two tooth pitch. The pitch point on the plots are represented at the time = 0 seconds. It must be noted that the pit located at the pitch point has the maximum effect on the static transmission error. Fig. 7 also shows that as the pit depth increase the variation in the magnitude of transmission error also increases. The effect of pit at the pitch point is higher when compared to the effect of pits at either side of pitch point. It can also be seen that the STE for damaged

locations is much higher than the STE for no damage. There were seven pits modeled on the tooth surface, whereas the STE is seen for only five locations. It clearly means that the other two pits, each farthest from pitch on both addendum and dedendum sides, do not come in contact with the corresponding gear tooth. Thus, the tooth damage placed at the root side and the tip side has no effect on the static transmission error. From Figure 7 it can also be seen that the second pit from the pitch point on the dedendum side creates much less static transmission error compared to the second pit from the pitch point on the addendum side.

Fig. 8 is composite plot showing the effect of both damage size (pit depth), and coefficient of friction on static transmission quantified using three different characterizations of transmission error. It has three rows of figures, in which the first row has two figures, a 3-D plot on the left showing the effect of tooth damage and coefficient of friction on STE quantified using the most common peak to peak transmission error (PSTE) method and the line graph next to it shows the percentage change in STE for pit depths ranging from minimum of zero to maximum of 0.127 mm. Likewise, rows two and three have the same 3-D plot on the left and a line graph on the right for STE quantified using root mean square

transmission error (RMSTE), and total area transmission error (TATE). While each analysis case simulated a single pit the results of several analyses, to study all of seven pit locations, are reported together and appear as one curve in the plots to follow. In order to see the effect of all pits starting from the root of pinion tooth to the tip of the tooth, a time of two base-pitch rotations has been used for processing the data in all three methods of STE calculation. For better comparison of results in Fig. 8, the ordinates are same for 3-D plots on the left and line graphs on the right. From the 3-D graphs on the left, regardless of the method used for STE quantification, STE increased with pit depth for all friction coefficients starting from zero to max. Furthermore, STE also increases with increase in coefficient of friction for all pit depths, but this increase is very small compared to the increase in STE due to increase in pit depth. In the line plots on the right column of Figure 8, it can be seen that as the friction increases from zero to max, the percentage increase in STE increases significantly higher when there is no damage on the tooth. However, this percentage change in STE reduces as pit depths increase from zero to max, indicating the effect of increase in damage size on STE is significantly greater than the effect of increase in friction.

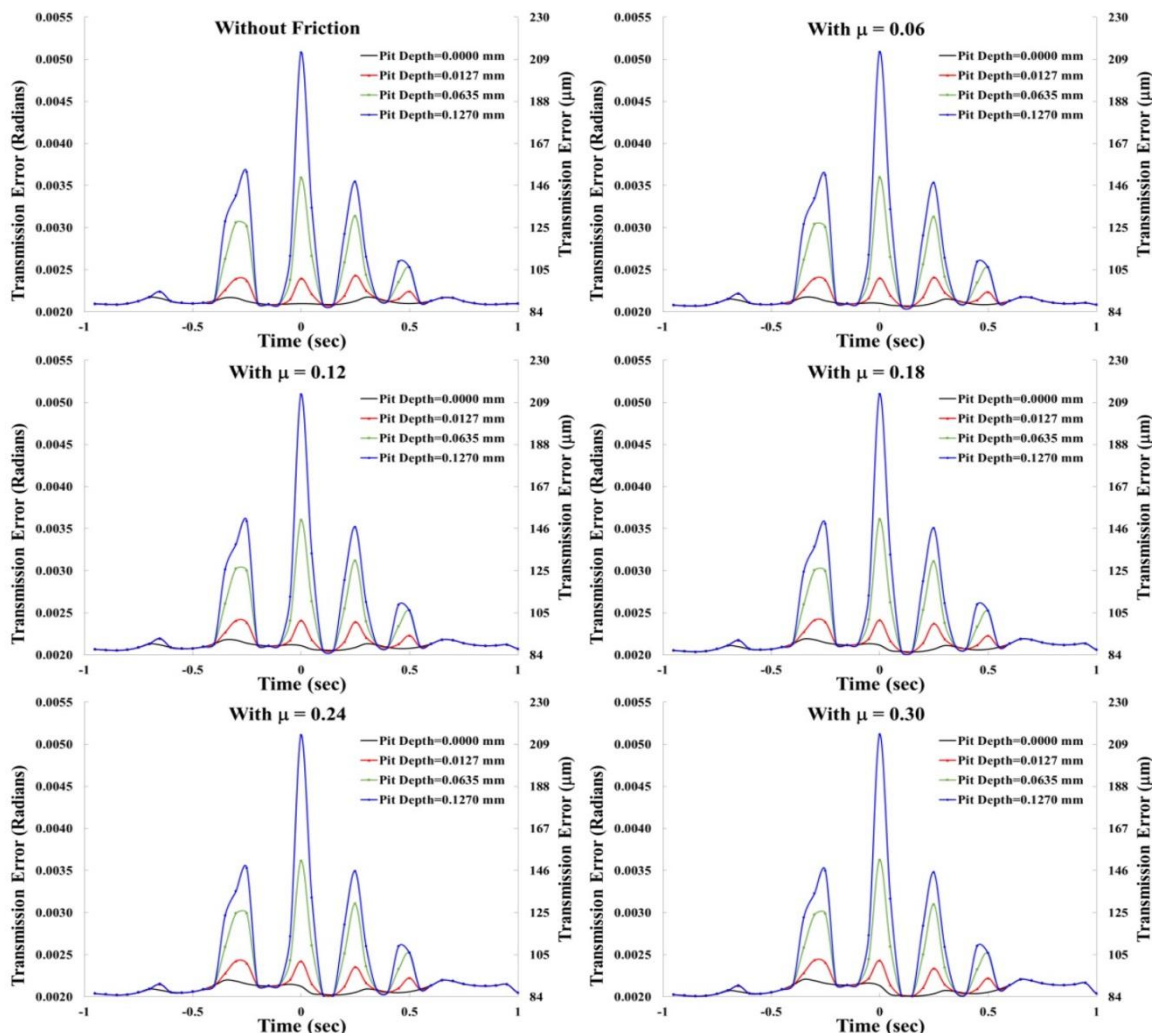


Figure 7. Transmission error variations at different pit shapes and friction coefficient

Comparing the three 3-D plots in Fig. 8, it is clear that peak-to-peak transmission error (PPTE) is much larger than the root mean square transmission (RMSTE), which is understandable that PPTE method just takes the magnitude of the distance between peak to valley, compared to the root mean square of several measurements as shown in Fig. 6. Likewise, if the entire area under the curve is used, the results total area transmission error (TATE) is even smaller than the RMSTE value. Regardless of the how STE is calculated, both tooth damage and friction increase STE. Furthermore, the effect of increase in pits size is significantly greater than the effect of increase in friction coefficient. Table II show the percentage change in STE when the coefficient of friction changes from zero to a maximum value of 0.3, for different values of pit depth and STE quantification method. When there is no damage i.e. when there are no pits, PPTE shows a 129% increase

in STE when friction changes from zero to 0.3. While RMSTE and TATE shows an increase of 123% and 42% respectively, when friction changes from zero to 0.3.

TABLE II. PERCENTAGE CHANGE IN STE WITH RESPECT TO STE QUANTIFICATION METHOD

	% Change in STE when μ Changes from 0.0 to 0.3			
	Pit Depth = 0.0000 mm	Pit Depth = 0.0127 mm	Pit Depth = 0.0635 mm	Pit Depth = 0.1270 mm
PPTE	129%	24%	8%	4%
RMSTE	123%	19%	1%	-1%
TATE	42%	9%	-2%	-3%

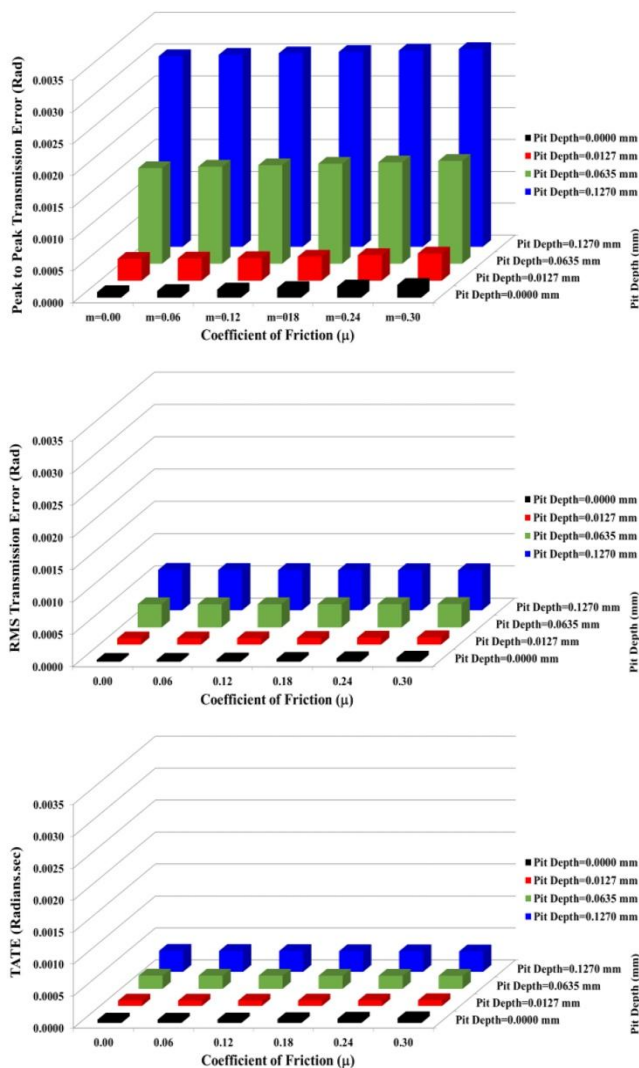
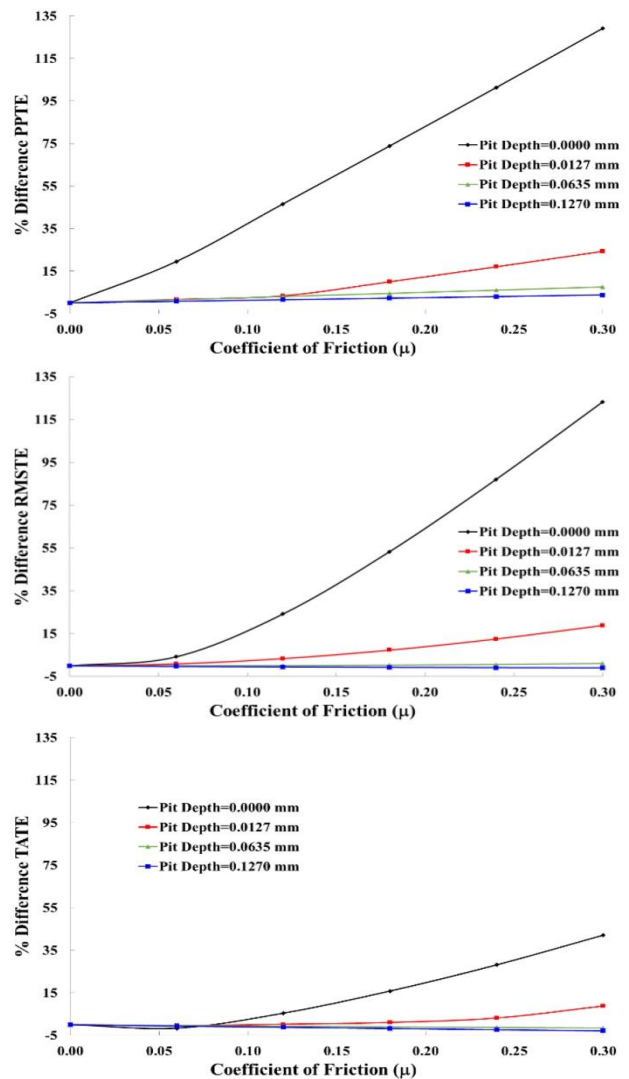


Figure 8. Comparison of STE with three different metrics at different coefficient of frictions

However, at the maximum pit depth of 0.127 mm, the PPTE shows only 4% increase in STE, while RMSTE and TATE show a decrease of 1% and 3% respectively. This is also seen in Fig. 9 for all values of friction coefficient. Although using peak to peak value for



calculation of STE is common, it is clear from Fig. 9 that using just the peak to peak value gives much higher values of STE compared to RMSTE and TATE values of Transmission Error. This effect become more significant as the surface damage size increases from zero to max, as

can be seen in figure 9 for maximum pit depth of 0.1270 mm.

In summary all data analysis results show a clear trend that the static transmission error in the gear systems

increase with increase in damage size and friction, but increase in damage size has a much greater effect on STE compared to increase in friction.

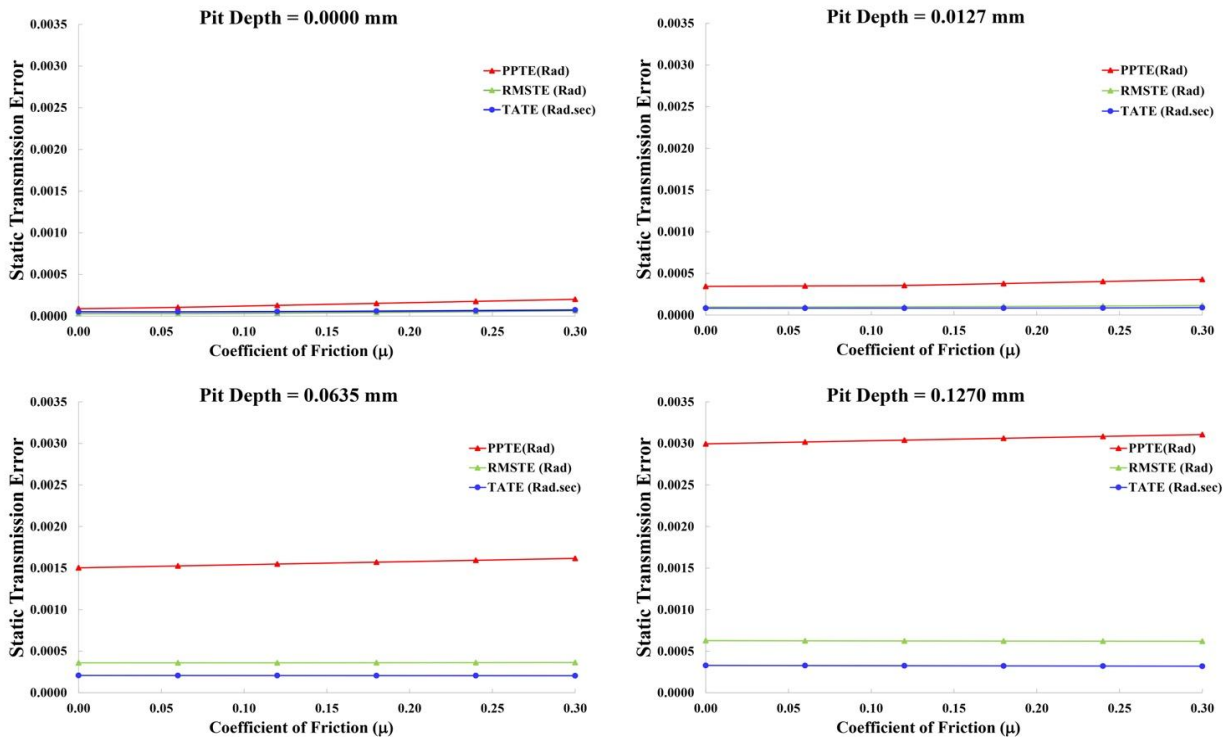


Figure 9. Comparison of static transmission error at different coefficient of frictions

V. CONCLUSIONS

1. Static transmission error increases with increases in pit depth.
2. The deepest pit has the most significant effect on static transmission error.
3. The pit located in the pitch region has the highest influence on static transmission error.
4. Farther the pit from the pitch point, either on addendum or dedendum side, lower is its effect on static transmission error.
5. Static transmission error increases with increase in coefficient of friction.
6. Effect of tooth damage in the form of pit depth is much higher than the effect of increase in coefficient of friction.
7. A combination of higher friction and larger pit depth results in the largest magnitude of static transmission error.

CONFLICT OF INTEREST

The work presented in this paper was carried out without any personal, professional or financial relationships that could potentially be construed as a

conflict of interest. Thus, the authors declare no conflict of interest.

AUTHOR CONTRIBUTIONS

Wasiq Abdul conducted all the simulation experiments with the help of Dr. Timothy Krantz, who provided the simulation software and guidance on how to use and interpret the results. Dr. Krantz also formulated the problem for investigation. Analysis results from Finite Element simulation work was discussed by everyone. Iqbal Shareef created the first draft of the paper, and served as the overall coordinator of manuscript internal review and updating of the manuscript after each review. He also served as the corresponding author for the IJMERR. All authors reviewed and approved the final version.

ACKNOWLEDGMENT

The authors would like to thank NASA Glenn Research Center, Bradley University, and Advanced Numerical Solutions Hilliard, Ohio. Partial support for this work in the form of graduate assistantship was from Dr. Jeffrey Bakken, Dean of Graduate School at Bradley University.

REFERENCES

- [1] B. Giorgio, and F. Pellicano. "Non-smooth dynamics of spur gears with manufacturing errors," *Journal of Sound and Vibration*, vol. 306, no. 1-2, 2007, pp. 271-283.

- [2] C. Fakher, T. Fakhfakh, R. Hbaieb, J. Louati, and M. Haddar, "Influence of manufacturing errors on the dynamic behavior of planetary gears," *The International Journal of Advanced Manufacturing Technology*, vol. 27, no. 7-8, 2006, pp. 738-746.
- [3] R. Kasuba, and J. W. Evans, "An extended model for determining dynamic loads in spur gearing," *Journal of Mechanical Design*, vol. 103, no. 2, 1981, pp. 398-409.
- [4] Wirtz, F. Sebastian, N. Beganovic, P. Tenberge, and D. Söffker, "Frequency-based damage detection of spur gear using wavelet analysis," In *Proc.c 8th European Workshop on Structural Health Monitoring (EWSHM 2016)*, pp. 5-8. 2016.
- [5] Jia, S. X., and I. Howard, "Comparison of localised spalling and crack damage from dynamic modelling of spur gear vibrations," *Mechanical Systems and Signal Processing*, vol. 20, no. 2, 2006, pp. 332-349.
- [6] M. Rui, and Y. S. Chen, "Research on the dynamic mechanism of the gear system with local crack and spalling failure," *Engineering Failure Analysis*, vol. 26, 2012, pp. 12-20.
- [7] Z. G. Wan, H. R. Cao, Y. Y. Zi, W. P. He, and Z. J. He, "An improved time-varying mesh stiffness algorithm and dynamic modeling of gear-rotor system with tooth root crack," *Engineering Failure Analysis*, vol. 42, 2014, pp. 157-177.
- [8] C. Q. Hu W. A. Smith, R. B. Randall, and Z. X. Peng, "Development of a gear vibration indicator and its application in gear wear monitoring," *Mechanical Systems and Signal Processing*, vol. 76, pp. 319-336, 2016.
- [9] M. Hui, Z. W. Li, M. J. Feng, R. J. Feng, and B. C. Wen, "Time-varying mesh stiffness calculation of spur gears with spalling defect," *Engineering Failure Analysis*, vol. 66, pp. 166-176, 2016.
- [10] R. Hbaieb, F. Chaari, T. Fakhfakh, and M. Haddar, "Influence of eccentricity, profile error and tooth pitting on helical planetary gear vibration," *Machine Dynamics Problems*, vol. 29, no. 3, 2005, pp. 5-32.
- [11] R. B. Randall, "A new method of modeling gear faults," *Journal of Mechanical Design*, vol. 104, no. 2, 1982, pp. 259-267.
- [12] P. D. McFadden, "Examination of a technique for the early detection of failure in gears by signal processing of the time domain average of the meshing vibration," *Mechanical systems and signal processing*, vol. 1, no. 2, 1987, pp. 173-183.
- [13] P. D. McFadden, "Determining the location of a fatigue crack in a gear from the phase of the change in the meshing vibration," *Mechanical Systems and Signal Processing*, vol. 2, no. 4, 1988, pp. 403-409.
- [14] Zakrajsek, J. James, F. R. Handschuh, D. G. Lewicki, and H. J. Decker, "Detecting gear tooth fracture in a high contact ratio face gear mesh," 1995.
- [15] F. K. Choy, V. Polyshchuk, J. J. Zakrajsek, R. F. Handschuh, and D. P. Townsend, "Analysis of the effects of surface pitting and wear on the vibration of a gear transmission system," *Tribology international*, vol. 29, no. 1, 1996, pp. 77-83.
- [16] J. H. Kuang, and A. D. Lin, "The effect of tooth wear on the vibration spectrum of a spur gear pair," *Journal of Vibration and Acoustics*, vol. 123, no. 3, 2001, pp. 311-317.
- [17] P. J. Dempsey, Gear damage detection using oil debris analysis, 2001.
- [18] H. Ian, S. X. Jia, and J. D. Wang, "The dynamic modelling of a spur gear in mesh including friction and a crack," *Mechanical systems and signal processing*, vol. 15, no. 5, 2001, pp. 831-853.
- [19] Decker, Harry J. Gear crack detection using tooth analysis. No. ARL-TR-2681. Army Research Lab, Cleveland OH, 2002.
- [20] L. Lin, and D. J. Pines, "The influence of gear design parameters on gear tooth damage detection sensitivity," *Journal of mechanical design* vol. 124, no. 4, 2002, pp. 794-804.
- [21] C. Gosselin, "The effects of localized gear tooth damage on the gear dynamics-a comparison of the effect of a gear tooth root crack and a spall on the gear transmission error," *Vibrations in Rotating Machinery*, vol. 16, no. 333, 2004.
- [22] F. Chaari, T. Fakhfakh, and M. Haddar, "Dynamic analysis of a planetary gear failure caused by tooth pitting and cracking," *Journal of Failure Analysis and Prevention*, vol. 6, no. 2, 2006, pp. 73-78.
- [23] R. Hbaieb, F. Chaari, T. Fakhfakh, and M. Haddar, "Influence of eccentricity, profile error and tooth pitting on helical planetary gear vibration," *Machine Dynamics Problems*, vol. 29, no. 3, 2005, pp. 5-32.
- [24] S. Vijayakar, "Multi-body dynamic contact analysis tool for transmission design" – *SBIR Phase II Final Report, ARL CR-487*, 2003.
- [25] S. Vijayakar, "Helical3D validation manual," Advanced Numerical Solutions, 3962 Brown Park Dr # C, Hilliard, OH 43026, 2005, pp. 1-176
- [26] Krantz, L. Timothy, "Gear tooth stress measurements of two helicopter planetary stages," NASA Technical Memorandum 105651, AVSCOM Technical Report 91-C-038 (1992).
- [27] L. Haris, "Impact of system-level factors on planetary gear set behavior," PhD diss., The Ohio State University, 2007
- [28] A. Kahraman, H. Ligata, and A. Singh, "Influence of ring gear rim thickness on planetary gear set behavior," *Journal of Mechanical Design*, vol. 132, no. 2, 2010, p. 021002.
- [29] P. E. Prueter, "A Study of the Mechanical Design and Gear Tooth Root Strains in Flexible Pin, Multi-Stage," Planetary Wind Turbine Gear Trains Using Three Dimensional Finite Element/Contact Mechanics Models and Experiments (Doctoral dissertation, The Ohio State University), 2011.
- [30] P. E. Prueter, R. G. Parker, F. Cunliffe, "A study of gear root strains in a multi-stage planetary wind turbine gear train using a 3-D finite element/contact mechanics model and experiments," In ASME Power Transmission and Gearing Conference, Washington, DC, p. DETC2011-47451, 2011.
- [31] T. M. Ericson, R. G. Parker, "Planetary gear modal vibration experiments and correlation against lumped-parameter and finite element models," *Journal of Sound and Vibration*, vol. 332, no. 9, pp. 2350-2375, 2013.
- [32] R. G. Parker, S. M. Vijayakar, and T. Imajo, "Non-linear dynamic response of a spur gear pair: modelling and experimental comparisons," *Journal of Sound and Vibration* 237, no. 3, 2000, pp. 435-455.
- [33] A. Kahraman, and G. W. Blankenship, "Effect of involute tip relief on dynamic response of spur gear pairs," *Journal of Mechanical Design*, vol. 121, no. 2, 1999, pp. 313-315.
- [34] M. Beghini, G. M. Bragallini, F. Presicce, and C. Santus, "Influence of the linear tip relief modification in spur gears and experimental evidence," in *Proc. ICEM12*, September (2004).
- [35] Tamminana, V. Krishna, A. Kahraman, and S. Vijayakar, "A study of the relationship between the dynamic factors and the dynamic transmission error of spur gear pairs," *Journal of Mechanical Design*, vol. 129, no. 1, 2007, pp. 75-84.
- [36] W. A. Abdul, T. L. Krantz, I. Shareef, "Influence of tip modification on performance characteristics of involute spur gears," *Australian Journal of Mechanical Engineering*, pp. 1-20, 2018.

Copyright © 2020 by the authors. This is an open access article distributed under the Creative Commons Attribution License (CC BY-NC-ND 4.0), which permits use, distribution and reproduction in any medium, provided that the article is properly cited, the use is non-commercial and no modifications or adaptations are made.

Dr. Iqbal Shareef is a professor of Industrial and Manufacturing Engineering at Bradley University, Peoria Illinois USA. He has BS, MS, PhD and postdoctoral research in Mechanical Engineering. During his tenure at Bradley, he has taught graduate and undergraduate courses in areas of Manufacturing Processes, Design for Manufacturing, Optimal Design, and Tribology. He has more than 70 publications. He is a Registered Professional Engineer in the state of Illinois and as a member of NCEES he has written more than 100 PE questions. He is a member of ASM, ASME, SME, TMS, ISPE, NSPE, Tau Beta Pi, and Sigma Xi.

Dr. Timothy L. Krantz has worked since 1987 as a research engineer at the NASA Glenn Research Center. He has researched many topics for power transmissions and spacecraft mechanisms, with an emphasis on helicopter gearbox technologies. His present roles at NASA includes member of the NASA Engineering Safety Center's Mechanical Systems Discipline Team, Technical Lead for the Revolutionary Vertical Lift Technology Project, and primary investigator for gearing experiments that supports an assessment of a mechanism for the James Webb Space Telescope. Dr. Krantz is a Fellow of the American Society of Mechanical Engineers.

Wasiq A.M. Abdul is a graduate research assistant in the department of Industrial and Manufacturing Engineering and Technology at Bradley University, Peoria Illinois, USA, and a certified manufacturing engineer (CMfgE). He holds a bachelor of science degree in mechanical engineering and is currently pursuing a masters in manufacturing engineering. His research interests include design and analysis of spur gears with tip relief modifications, analysis of damaged gears with friction, analysis of gear spacing errors in planetary systems, Six Sigma to optimize surface roughness and design for manufacturability.